AJNR

Dyke Award Paper. Kinetics of pathologic blood-brain-barrier permeability in an astrocytic glioma using contrast-enhanced MR.

U P Schmiedl, J Kenney and K R Maravilla

AJNR Am J Neuroradiol 1992, 13 (1) 5-14
http://www.ajnr.org/content/13/1/5

Dyke Award Paper

Kinetics of Pathologic Blood-Brain-Barrier Permeability in an Astrocytic Glioma Using Contrast-Enhanced MR

Udo P. Schmiedl,[1] James Kenney,[1] and Kenneth R. Maravilla[1]

Purpose: The feasibility of measuring blood-brain barrier permeability was studied in a 36B-10 brain glioma model in rats. **Materials and Methods:** In stage I of our study, sequential MR images of glioma-implanted rats were obtained following intravenous administration of three contrast agents of different molecular sizes—Gd-DTPA, polylysine-(Gd-DTPA), and albumin-(Gd-DTPA). In a second set of experiments, sequential MR imaging with Gd-DTPA, quantitative measurements of plasma Gd-DTPA concentration, and postmortem tumor Gd-DTPA measurements were used to estimate the blood-to-tissue transport coefficient (K_i) in the rat glioma model at 11 and 15 days postimplantation. **Results:** In stage I, Gd-DTPA caused rapid and greatest tumor enhancement with a significant washout from the tumor during the 120-min experiment. Tumor enhancement using polylysine-(Gd-DTPA) occurred later and was significantly less compared to Gd-DTPA. Tumor signal intensity increased only slowly over time and the peak level of enhancement was least using albumin-(Gd-DTPA). In stage II, the mean (±1 SD) K_i values were 1.1 ± .24 at 11 days, and 9.3 ± .8 at 15 days postimplantation. These results correspond well with published data obtained by autoradiography. **Conclusion:** We believe that the differential enhancement pattern using contrast agents of different molecular sizes reflects a differential permeability of the pathologic blood-brain barrier, and that our studies demonstrate the feasibility of using frequent sequential images and a graphical approach to K_i calculation to determine the blood-to-tissue transport coefficient using contrast-enhanced MR.

Index terms: Blood-brain barrier; Magnetic resonance, experimental studies; Glioma; Contrast media, paramagnetic

AJNR 13:5–14, January/February 1992

The capillary wall of most vessels outside the central nervous system (CNS) is, to a variable degree, permeable and allows free exchange between blood and interstitial fluid of electrolytes and molecules up to the size of albumin. In the CNS, the interface between the blood and the brain, known as the blood-brain barrier (BBB), functions like a semipermeable plasma cell membrane allowing water molecules to diffuse along osmotic gradients and to maintain iso-osmolality of solutes on either side of the BBB. Highly lipophilic, non-protein-bound substances that are nonionized at physiologic pH readily cross the BBB. For some solutes, including glucose, amino acids, monocarboxylic acids, and choline, specific transport mechanisms across the BBB have been identified (1, 2). Morphologically, the BBB consists of a thin sheet of endothelial cells that are closely apposed to each other and form tight junctional complexes. In addition to the tight junctions between capillary endothelial cells, there is a continuous basement membrane within these capillaries and a paucity of pinocytic transport vesicles within the endothelial cells that combine to further restrict the movement of most blood-borne substances into the brain (1, 2).

Alteration of the capillary endothelium by pathologic processes typically increases the permeability of the BBB. In brain tumors, the increased permeability of capillaries has been ascribed to induction of neovascularity with variably normal or abnormal endothelium (3, 4). In low-grade gliomas, such as grade 1 astrocytoma, the newly formed capillaries closely resemble normal cerebral capillaries with an intact BBB, while in more malignant tumors, capillaries are fenestrated and show in-

Received March 27, 1991; accepted and revision requested May 1; revision received July 3; final acceptance July 15.

Presented at the 29th Annual Meeting of the ASNR, Washington, DC, June 9–14, 1991.

[1] All authors: Department of Radiology, SB-05, University of Washington, Seattle, WA 98195. Address reprint requests to U. P. Schmiedl.

AJNR 13:5–14, Jan/Feb 1992 0195-6108/92/1301-0005

creased pinocytosis (3, 4). Often, in these tumors, basement membranes and glial foot processes are absent, allowing compounds as large as proteins and blood products to be taken up by astrocytes (1, 3, 4). This pathologic alteration of the BBB allows intravascular contrast agents that distribute within the extracellular fluid space to diffuse into and accumulate in brain lesions, whereas normal capillaries prevent passage of contrast agents into normal brain tissue. This feature has been widely used in diagnostic imaging modalities such as computed tomography (CT) and magnetic resonance (MR) imaging to increase the conspicuity of lesions through the use of intravascular contrast agents (1). It has been proposed that quantitative determination of BBB permeability would be of clinical value for purposes such as optimizing dose and delivery of chemotherapeutic agents to a given tumor. However, efforts to quantitate the permeability of the BBB in tumors using contrast-enhanced MR or CT have been very limited.

Therefore, we undertook a study to determine the potential of using MR imaging for noninvasive, high-resolution determination of BBB permeability. The objectives of our study were twofold. First, we tested the hypothesis whether larger molecules would transgress from blood into the tumor at a slower rate compared to small molecules, thereby reflecting the "leakiness" of tumor capillaries. Second, we attempted to quantitate the degree of BBB permeability using Gd-DTPA. Empirical calibration curves that allow the determination of tissue Gd-DTPA concentration from the image enhancement of the tumor were used in conjunction with sequential MR imaging and blood sampling to determine the blood-to-tissue transport constant, K_i, in these tumors.

Materials and Methods

Experiments were divided into two stages, each designed for a different purpose. The first stage was to determine whether the molecular size would affect the rate of passage of a contrast agent across the pathologic BBB in an experimental glioma model. The second stage was to study whether the blood-to-tissue transport coefficient (K_i) can be measured with MR by using one of the contrast agents to determine BBB permeability.

MR Technique

A 1.5 T clinical MR system (Signa, General Electric, Milwaukee, WI) was used for all imaging experiments.

For imaging studies comparing the three contrast agents of differing molecular size, a specially designed small animal holder and a 12.5-cm round surface coil were used, as described previously (Fig. 1) (5). Using this device, high resolution MR brain images of eight anesthetized rats can be obtained simultaneously. Briefly, the holder consists of two parts, one being the mirror image of the other. One part of the holder can hold four rats, with two opposing rats facing each other. The tapered, V-shaped design of each stall can hold rats up to 350 g in position without compromising their respiratory status. During the imaging procedure, four rats were positioned in the top half of the holder, and four rats were positioned supine in the bottom half. The surface coil is positioned between the upper and lower segments of the probe, such that the center of the coil is equidistant with respect to identical anatomical structures in the transverse, sagittal, and coronal plane of each rat head (5). The entire holder containing eight anesthetized rats is then placed in the center of the magnet. Test tubes containing commercial corn oil were placed centrally in the holder. Heads of the eight rats were imaged simultaneously using graphically prescribed multislice images utilizing a 10-cm field of view. With this approach, detailed images with directly comparable signal intensities of identical anatomical structures were obtained. A T1-weighted coronal multislice spin echo (SE) sequence (250/20/4) (TR/TE/excitations) with eight transverse slices is then obtained on each side of the center of the coil (slice thickness, 4 mm) covering the brain and the viscerocranium of each rat. A matrix of 256 × 192, was used which yields an in-plane pixel resolution of 0.4 × 0.5 mm on each side.

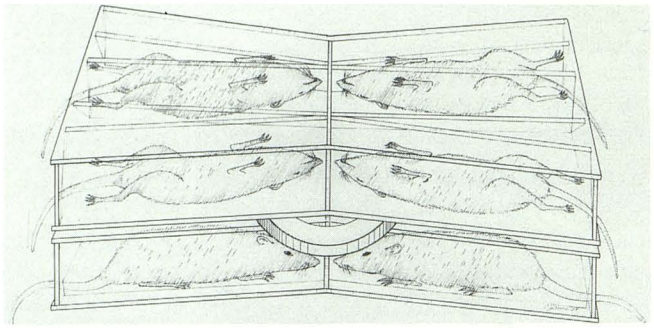

Fig. 1. Schematic drawing of the assembly showing six of eight rats, two rats in prone position in the bottom half and four rats in supine position in the top half of the probe. The surface coil is positioned between the two halves of the probe, equidistant to the heads of the eight rats.

In the second set of experiments, to further quantitate blood-to-tissue transport using Gd-DTPA, imaging was performed as single animal experiments on six rats between 11 and 15 days post-tumor implantation. These studies were performed using a 10-cm inner diameter wrist coil and an 8-cm field of view. A 256 × 128 matrix and a slice thickness of 4 mm yielded an in-plane resolution of 0.3 × 0.6 mm. Sequence parameters consisted of SE (233/23/4).

Animal Preparation

The brain tumor model used in the current study is well established at our institution and has been used extensively

to study permeability with QAR (6, 7). Twenty-six F-344 rats, male and female, weighing approximately 150–300 grams, were implanted with viable cells of the 36B-10 ethylnitrosourea-induced astrocytic glioma line using a previously described technique (6). These tumors typically grow to 0.06 grams in 16–20 days. Additionally these rats also develop subcutaneous tumors due to tumor cell implantation at the site of surgery.

For the stage I imaging experiments, 27-gauge scalp vein catheters were placed into the tail veins of each rat following anesthesia with intraperitoneal injection of 40–50 mg/kg pentobarbital before placing them in the animal holder and positioning them in the MR scanner. For the BBB quantitation experiments, femoral arterial lines were also inserted. The intravenous lines and arterial lines were accessible through open ends of the animal holder and coil so that contrast material can be administered to the rats or blood can be withdrawn during an experiment without changing the position of the rats.

Contrast Media

Gadopentetate dimeglumine (Gd-DTPA), diluted in 0.9% NaCl was administered at a dose of 0.2 mmol/kg. The doses of polylysine-(Gd-DTPA) and albumin-(Gd-DTPA) was adjusted to provide equal relaxivity effects when injected into the animals.

Polylysine-(Gd-DTPA) (Schering AG, Berlin, Germany) was synthesized by covalently binding Gd-DTPA molecules to a linear polymer of lysine molecules. The compound was dissolved in 0.9% NaCl at a concentration of 20 mmol Gd^{+3}/L. The average molecular weight of this compound was 48,000, the T1-relaxivity as measured at 39°C and 0.47 T was 13.1 $mmol^{-1}$ sec^{-1} per Gd^{+3} (G. Schuhman-Giampieri, PhD, Schering AG, Berlin, Germany, personal communication). Based on the Gd^{+3} content of the polylysine solution, doses of 0.07 mmol/kg and 0.35 mmol/kg were used. Albumin-(Gd-DTPA) (molecular weight = 91,000) (Schering AG) was synthesized by covalently binding Gd-DTPA molecules to human serum albumin, as previously described in detail, and administered intravenously at a dose of 0.06 mmol Gd^{+3}/kg (8). The T1 relaxivities (R1) of albumin-(Gd-DTPA) as measured at 39°C and 0.47 T was 15.3 $mmol^{-1}$ sec^{-1} per Gd^{+3} (G. Schuhman-Giampieri, PhD, personal communication). The comparative relaxivity effect of these solutions was verified by phantom experiments. The Gd^{3+} dose using albumin Gd-DTPA and the polylysine-(Gd-DTPA) (low dose) was approximately ⅓ of the dose employed with Gd-DTPA to compensate for the increased relaxation effectiveness (approximately 3×) of the Gd^{+3} ion when coupled to the polylysine or albumin molecules, respectively. Therefore, a similar relaxivity effect in vivo using low-dose polylysine-(Gd-DTPA) and albumin-(Gd-DTPA) compared to that obtained with Gd-DTPA was expected.

Comparison of Contrast Media

Following acquisition of precontrast images, Gd-DTPA (0.2 mmol/kg) (n = 4 rats), albumin-(Gd-DTPA) (0.06 mmol Gd/kg) (n = 7 rats), or polylysine-Gd-DTPA (0.07 mmol Gd/kg) (n = 5 rats) and 0.35 mmol Gd/kg (n = 4 rats)) was administered intravenously via tail vein catheters. Contrast material was administered to the rats simultaneously over 20 sec without changing the animals' positions with respect to the surface coil and lines were flushed with 1 mL of saline. Postcontrast images were obtained at 5, 15, 25, 35, 45, 60, 90, 105, and 120 min following injection. MR amplifier settings were held constant within each experiment. Region-of-interest (ROI) measurements were obtained over both hemispheres at the level of the thalami (100 pixels each), the intraaxial tumor (average 16pixels), the subcutaneous tumor (average 16 pixels), the cavernous sinus (9 pixels), and an oil phantom (25 pixels) that had been positioned centrally in the imaging probe at the level of the rats' brains. ROIs were identical in size and location for a particular anatomical structure on subsequent images.

Intensity data were normalized to the external standard and are presented as a mean, ±1 SD, on an arbitrary linear scale. Differences between signal intensities were assessed for significance by means of the paired Student's *t*-test. Scores of $P < .01$ were considered significant.

Quantitation of Blood-to-Tissue Transport

Following acquisition of the precontrast image, an infusion of 0.15 M Gd-DTPA was begun, at a rate of 0.05 mL/min in animals weighing 250–350 g and 0.025 mL/min in those weighing 150–250 g. The time at the start of the infusion was defined as t = 0, and simultaneously with Gd-DTPA infusion, sequential arterial blood samples and images were acquired. Removed blood (0.25 mL per sample) was replaced with heparinized saline. Blood was drawn every 2 min for 16 min, then at 21, 26, 36, 46, and 54 min or accordingly shorter periods, depending on the duration of the experiments (Table 1). Images were obtained every 2 to 3 min for the first 30 min of the experiment, and about every 10 min thereafter.

Four of the six experiments were terminated at 10, 20, 40, and 54 min postinjection to determine the Gd^{+3} content in the tumors. These four animals were sacrificed following the last image, and their brains were immediately frozen in liquid N_2 and stored at −4°C for determination of tumor tissue (Gd-DTPA). The purpose of this was to generate calibration plots that would give tissue (Gd-DTPA) as a function of image enhancement.

ROI measurements were obtained for each image over the intraaxial tumor. ROIs were chosen to include the area

TABLE 1: Animal's designation, days postimplant, the duration of the experiment in min (Dur), the number of points (Npts) used in determining K_i, K_i (mL/kg · min), the confidence interval of K_i, and the intercept

Rat	Day	Dur	Npts	K_i	Confidence Interval	Intercept
A	11	40	7	0.6	0.4–0.9	−0.68
B	15	54	12	8.9	6.2–12.5	−44.7
C	15	20	9	9.6	6.7–13.4	−8.5
D	11	54	12	1.3	0.9–1.8	0.89
E	11	10	5	0.7	0.4–1.0	3.9
F	11	20	7	1.6	1.1–2.2	0.53

of tumor enhancement. Tumor enhancement was slightly heterogeneous in several instances. Since heterogeneous enhancement may indicate heterogeneous capillary permeability across the tumor section, we, therefore, likely averaged permeability in these tumors. For each postcontrast image, signal intensity was normalized to an external oil phantom and tumor enhancement was determined as the fractional increase in image intensity of the tumor relative to the precontrast image intensity.

Plasma (Gd-DTPA) Measurement

Samples were diluted 40 times with water, and gadolinium concentration was measured using inductively coupled plasma atomic emission spectroscopy (ICP-AES). ICP-AES standards were prepared by adding Gd-DTPA to a 40-fold dilution of normal rat plasma.

Tissue [Gd-DTPA] Measurement

The tumors were grossly excised, weighed, homogenized with 2.7–4.0 mL of water, and centrifuged. Gadolinium content in the supernatant was measured by ICP-AES, using a normal brain extract blank and standards prepared from Gd-DTPA and distilled water. A second extraction with 1.9 mL of water was performed on the pellet from the first extraction, and also analyzed by ICP-AES. Rarely, the second extraction contained a significant amount of gadolinium and its contribution was then included in the total tissue gadolinium content. To validate this method of tissue gadolinium measurement, four "sham" samples were prepared consisting of Gd-DTPA injected directly into normal brain tissue. These samples contained 568, 585, 581, and 556 μmol/kg Gd-DTPA; each weighed about 0.085 g. The sham samples were homogenized and analyzed by using ICP-AES as described above, using only a single extraction.

BBB Permeability Calculation

The blood-to-tissue transport constant K_i was calculated using the graphical method of Patlak et al (9). Details are summarized in the Appendix.

Results

As confirmed by autopsy after imaging, all rats developed grossly visible intraaxial and subcutaneous masses at the site of implantation. Subcutaneous tumors and intraaxial tumors were separated by normal brain tissue, dura, and the skull.

Comparison of Contrast Media

Intraaxial tumors typically were isointense or slightly hypointense compared to normal brain parenchyma on precontrast images (Fig. 2). Normal brain was not significantly enhanced with any of the contrast agents. Figure 3 shows the average signal intensity vs time as measured over the intraaxial tumors for the three contrast agents. Peak enhancement was achieved between 6 and 12 min p.i. (140% enhancement over baseline) using Gd-DTPA. Using the low dose of polylysine-(Gd-DTPA), no significant enhancement was observed in either the intraaxial or the subcutaneous tumors. With the higher dose of polylysine-(Gd-DTPA), a slowly increasing slope of signal enhancement in intraaxial tumors was observed that peaked (81% enhancement over baseline) between 24 and 30 min p.i. and decreased thereafter (Fig. 3). Enhancement of subcutaneous tumors using the high dose polylysine-(Gd-DTPA) peaked slightly earlier between 18 and 24 min (130% enhancement over baseline). In all cases, subcutaneous tumors showed greater peak enhancement levels compared to the intraaxial tumor both with Gd-DTPA and with polylysine-(Gd-DTPA) (Fig. 4).

The pattern of enhancement using albumin-(Gd-DTPA) differed in both the intraaxial and the subcutaneous tumors from the pattern of enhancement observed with Gd-DTPA and polylysine-(Gd-DTPA). Signal intensity using albumin-(Gd-DTPA) increased slowly over time in both tumor locations and there was significantly less enhancement compared to Gd-DTPA and polylysine-(Gd-DTPA). No peak enhancement was observed for the intraaxial tumor sites during the time period of the experiment (approximately 2 hr) using albumin-(Gd-DTPA). Tumor enhancement was greatest at 120 min in intraaxial tumors (52% over precontrast levels) and at 105 min in subcutaneous tumors (22% over precontrast levels).

On precontrast images, the cavernous sinus region had a low signal intensity compared to normal brain (Fig. 5). Signal enhancement in the cavernous sinus following administration of contrast media showed considerable variation between animals. Peak enhancement using Gd-DTPA (243% over precontrast levels), low-dose polylysine Gd-DTPA (116% over precontrast levels), and high-dose polylysine-(Gd-DTPA) (168% over precontrast levels) was measured between 6 and 18 min postinjection. Signal intensities decreased thereafter. Enhancement of slow-flowing blood using albumin-(Gd-DTPA) reached a plateau at 12 min p.i. (95% over precontrast levels) and remained fairly constant during the duration of the experiment.

Validation of Technique for Tissue [Gd] Determination

For the 4 sham tissue samples, which contained a mean of 572.5 μmol/kg Gd-DTPA, homogenization and ICP-AES analysis yielded a mean concentration value of 573 μmol/kg.

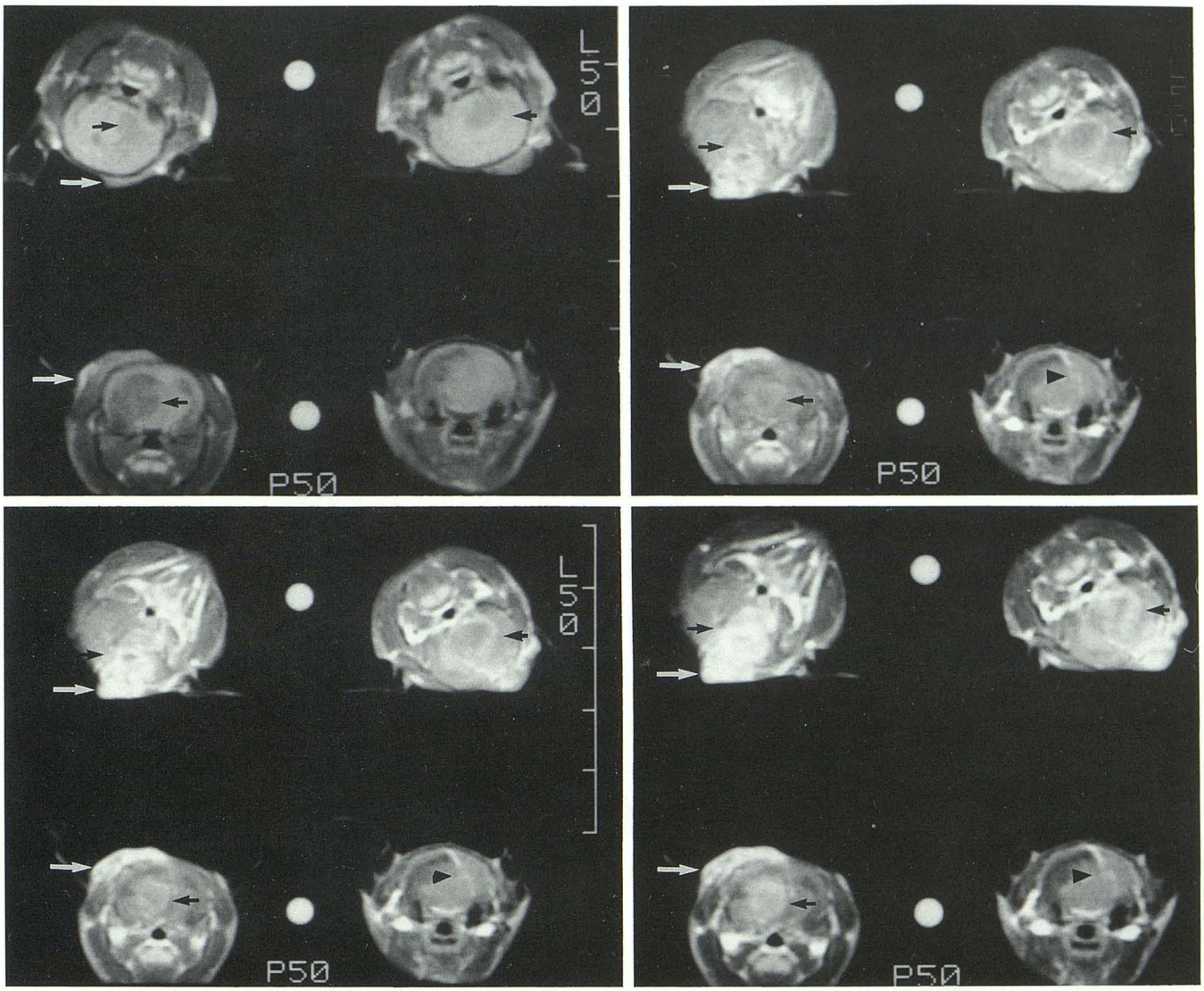

Fig. 2. *A–D*, Representative coronal SE (250/20/4) images of four rats with gliomas before (*A*), at 6 min (*B*), at 18 min (*C*), and at 90 min (*D*) following intravenous administration of polylysine-(Gd-DTPA) (0.035 mmol Gd/kg) and albumin-(Gd-DTPA) (0.06 mmol Gd/kg). No change in signal intensity was visible between 90 and 120 min. The two rats positioned to the left of the oil standard received polylysine-(Gd-DTPA), the two rats to the right of the oil standard received albumin-(Gd-DTPA). Using polylysine-(Gd-DTPA), intraaxial (*short arrow*), located in either cerebral hemisphere, and subcutaneous tumors (*long arrow*) show earlier and greater enhancement as compared to albumin-(Gd-DTPA). Due to the slice selection in this particular set of images, images of the rat on the bottom right that received albumin-(Gd-DTPA) only show the needle tract from the tumor implantation seen only as a linear lesion of increased signal intensity on postcontrast images (*arrowhead*). One rat (*top left*) in this set moved slightly between the preconstrast and postcontrast image acquisitions. The corresponding level was present on another slice of this sequence.

MR Enhancement Calibration

The tumors removed for calibration of MR enhancement to tissue [Gd-DTPA] weighed between 0.0088 and 0.1122 g, and contained Gd-DTPA concentrations between 21.25 μmol/kg and 388.4 μmol/kg. The double logarithmic calibration plots relating tissue Gd concentration to fractional image enhancement, fitted to lines using least-squares regression, yielded a linear relationship between the tissue Gd concentration and the image enhancement. The tissue Gd concentration (A) in μmol/kg is related to enhancement as follows: where $A = 64E^{2.29}$, and E = fractional tumor enhancement (confidence interval −30%/+40%). These intervals correspond to ± 1 SD in the natural log of the tissue Gd concentration.

Blood-to-Tissue Transport Constants

Table 1 shows K_i values and confidence intervals for each animal, as well as the values of the intercept for those animals for which the graphical approach was used. The K_i confidence interval

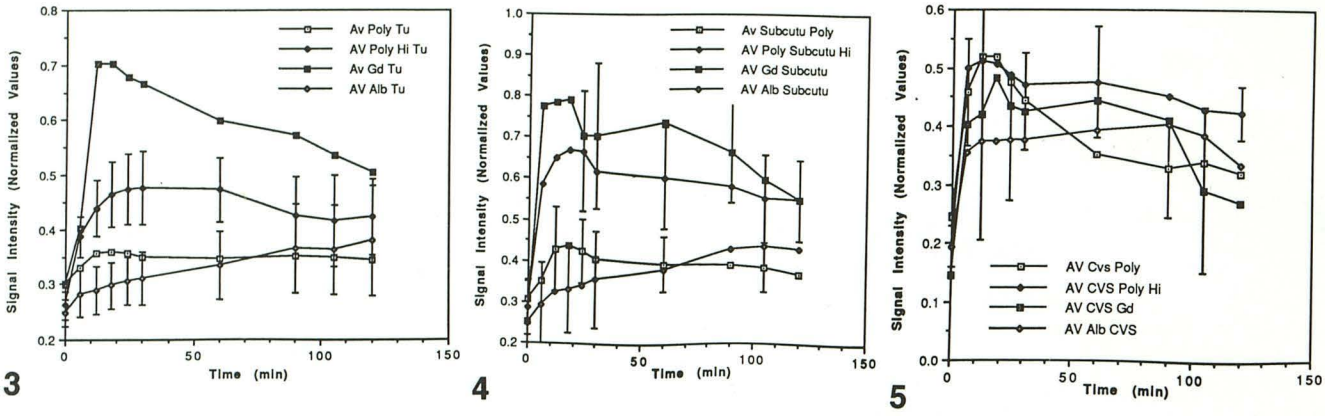

Fig. 3. Average signal intensity ±1 SD (representative) over time as measured in intraaxial gliomas following administration of polylysine-(Gd-DTPA) (0.07 mmol Gd/kg) (AvPolyTu), polylysine-(Gd-DTPA) (0.035 mmol Gd/kg) (AvPolyHiTu), Gd-DTPA (0.2 mmol/kg) (AvGdTu), and albumin-(Gd-DTPA) (0.06 mmol Gd/kg) (AvAlbTu). The graphs show different enhancement kinetics observed with the different contrast agents.

Fig. 4. Average signal intensity ±1 SD (representative) over time as measured in subcutaneous glioma tumors following administration of polylysine-(Gd-DTPA) (0.07 mmol Gd/kg) (AvSubcutu Poly), polylysine-(Gd-DTPA) (0.035 mmol Gd/kg) (Av polySubcutu Hi), Gd-DTPA (0.2 mmol/kg) (AvGd Subcutu), and albumin-(Gd-DTPA) (0.06 mmol Gd/kg) (AvAlbSubcutu). Contrast agents of different size show different enhancement kinetics.

Fig. 5. Average signal intensity ±1 SD (representative) over time as measured in the cavernous sinus following administration of polylysine-(Gd-DTPA) (0.07 mmol Gd/kg) (AvCVSPoly), polylysine-(Gd-DTPA) (0.035 mmol Gd/kg) (AvCVSPolyHi), Gd-DTPA (0.2 mmol/kg) (AvCVSGd), and albumin-(Gd-DTPA) (0.06 mmol Gd/kg) (AvAlbCVS). The graphs shows persistent enhancement of slow flowing blood for albumin-(Gd-DTPA) and the high dose of polylysine-(Gd-DTPA). This likely reflects the prolonged intravascular half life of the high molecular weight contrast agents.

corresponds to ±1 of Ln(K_i), based on the variance of tissue [Gd-DTPA] values obtained from the calibration curves. The intercepts of the linear portions of the curves ranged from −40 to +11 mL/kg, but in most instances were not significantly different ($P < .05$) from zero. They, therefore, do not represent, as expected from the distribution volume of Gd-DTPA, the plasma volume of the tumor.

The underlying graphs for the K_i calculation for rat D are shown in Figures 6–8. Figure 9 shows the corresponding images. The slope of the plot Apt/Cpt vs $\int_0^t C_{pt'dt'}/C_{pt}$ (Fig. 7), using the first 12 points, is $K_i = 1.3$ mL/kg-min.

The mean (±SEM) values of K_i for animals imaged at 11 days and 15 days postimplantation were 1.1 ± 0.24, and 9.3 ± 0.8 mL/kg·min, respectively.

Discussion

In this study, we compared the effects on MR imaging using contrast media of different molecular size in a brain glioma model. With increasing molecular size of contrast media, a slower and less intense tumor enhancement over time was observed The smallest molecule, Gd-DTPA caused early and greatest tumor enhancement, whereas with the intermediate sized molecule, polylysine-(Gd-DTPA), tumor enhancement was slower and less intense. The largest molecule, albumin-(Gd-DTPA), accumulated in the tumor even slower and showed a lesser total enhancement.

It is well established, that the major pharmacologic basis for tumor enhancement in the CNS using extracellular fluid contrast agents such as Gd-DTPA is largely due to dysfunctional BBB and leakage of the contrast agent into the interstitial space (10, 11). The different tumor enhancement kinetics for the three contrast agents used in the current study probably reflects differential permeability of tumor capillaries for large and small molecules, although other factors have to be taken into consideration. In highly vascular tumors, part of the enhancement may, at least in the initial phase of contrast media distribution, also be ascribed to blood-pool enhancement. Albumin-(Gd-DTPA) has been mostly used as an experimental prototype MR contrast agent to study blood-pool and perfusion-dependent contrast enhancement and to estimate tumor vascular space (12, 13). The slowly increasing slope of signal intensity in the tumor using albumin-(Gd-DTPA), however, indicates that the molecule slowly leaks from the intravascular space into the interstitium of the tumor. If the tumor enhancement were due to blood pool accumulation of albumin-(Gd-DTPA), an earlier and more rapid increase of tumor signal intensity would be expected. It is also known from other studies, that human serum albumin, in its course of repeated recirculation through tumor

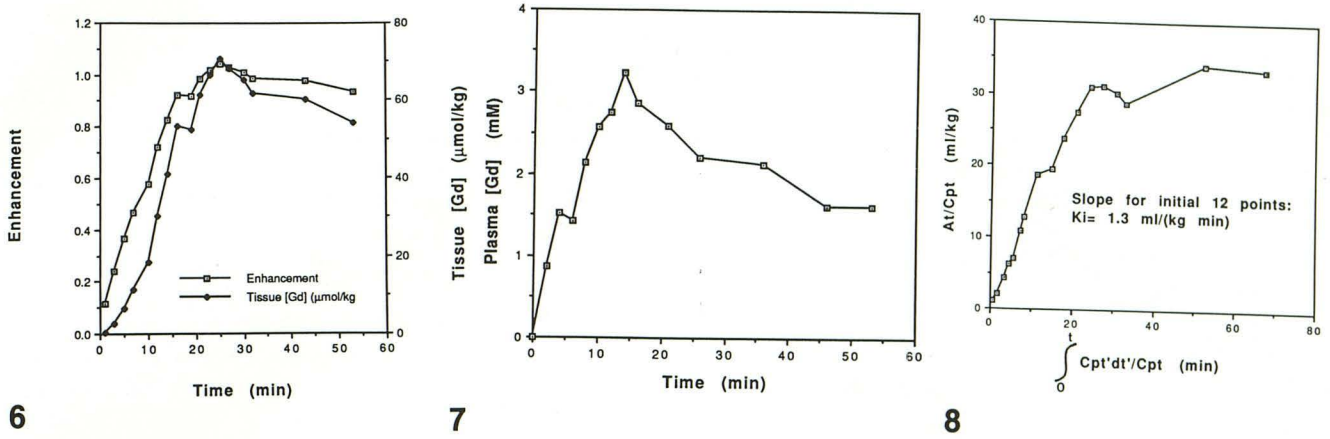

Fig. 6. Image enhancement and tumor tissue Gd^{+3} (derived from enhancement using the empirically determined relationship $A = 64E^{2.29}$) concentration over time as measured in rat D (Table 1).

Fig. 7. Plasma Gd^{+3} concentration over time as measure in rat D (see also Table 1). Gd^{+3} concentration increases, as expected, during infusion and decreases once the infusion of the contrast agent is ended.

Fig. 8. At/Cpt vs $\int_0^t C_{pt'}dt'/C_{pt}$ for rat D. Apt = tissue Gd^{+3} concentration at time t. Cpt = plasma Gd^{+3} concentration at time t.

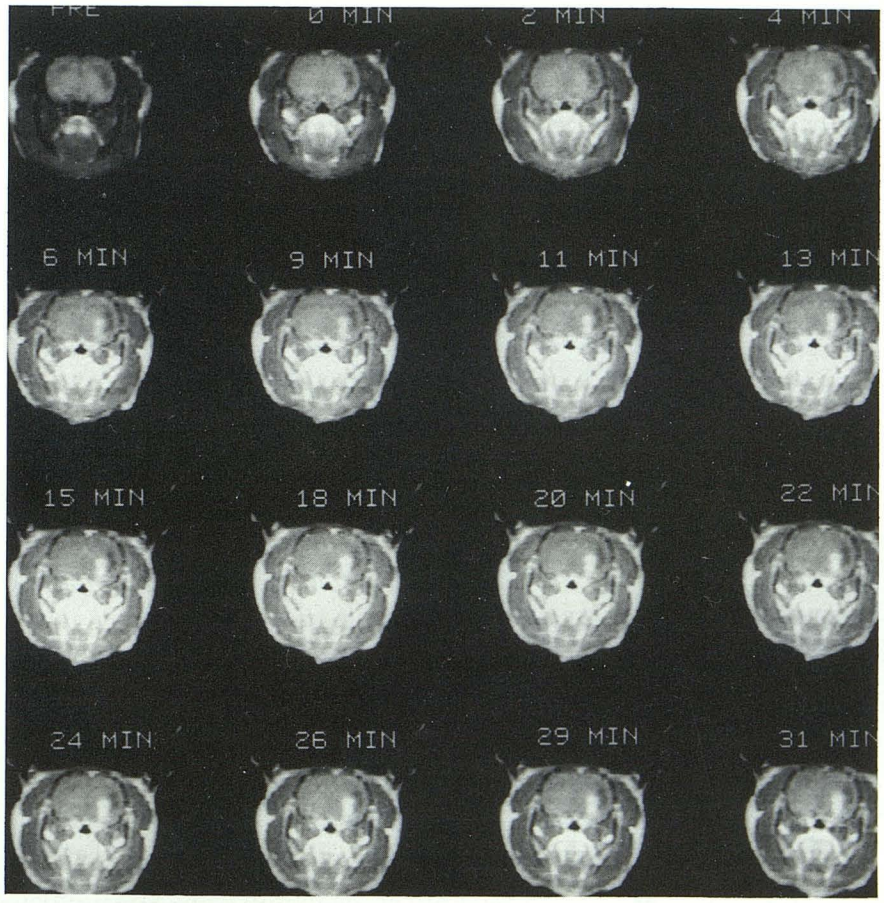

Fig. 9. Sequential coronal SE (233/23/4) images of rat D acquired before and during intravenous infusion of Gd-DTPA. On images selected from the initial 31 min of the experiment, the intraaxial glioma seen as a brightly enhancing lesion in the left hemisphere increases over time.

capillaries, may leak into the interstitium of tumors (13, 14).

Polylysine-(Gd-DTPA) is a relatively new experimental contrast agent designed to distribute, similarly to albumin-(Gd-DTPA), primarily within the intravascular space following intravenous injection. The intravascular half life of this molecule, however has been indicated to be significantly shorter compared to albumin-(Gd-DTPA) (G. Schuhman-Giampieri, PhD, personal communication) (15). In our study, signal intensity in tumors using the higher dose of polylysine-(Gd-DTPA) reached a plateau

between 30 and 60 min postinjection and decreased thereafter. The delayed and lower enhancement achieved with this contrast agent as compared to Gd-DTPA, seems to indicate that the tumor is less accessible for this contrast agent as compared to Gd-DTPA and that the rate limiting factor for the tumor enhancement is vascular permeability.

We did not directly study the possibility of dissociation of the Gd-DTPA molecule from either macromolecule. A slow release of Gd-DTPA from the macromolecular complex could, in theory, also explain the different enhancement kinetics observed in our study. This possibility seems, however very unlikely since Gd-DTPA is covalently bound to both albumin and polylysine, suggesting that both complexes, albumin-(Gd-DTPA) and polylysine-(Gd-DTPA), are relatively stable (8).

The downslope of the enhancement curve measured in tumors with Gd-DTPA clearly indicates, as expected, washout of the contrast agent from the tumor. Although the downslope of the enhancement curve using the higher dose of polylysine-(Gd-DTPA) may suggest that there was some washout of the contrast agent from the tumor, the difference between the maximum enhancement and the enhancement measured at 120 min p.i. was not significant. The relative persistent tumor enhancement using polylysine-(Gd-DTPA) seems to indicate that the contrast agent may be trapped in the tumor, a finding that is supported by the investigations of others who have reported binding of polylysine-(Gd-DTPA) to glioma cells both in culture and in an animal model (16, 17).

In the second part of the study, we chose the small molecule Gd-DTPA to further assess whether abnormal BBB leakiness could be quantified using MR. Gd-DTPA was chosen, because it has a similar distribution pattern as ^{68}Ga-EDTA, a radiotracer used in positron emission tomography studies to determine vascular permeability (18). Furthermore, Gd-DTPA is a clinically approved contrast agent, which would greatly facilitate its potential clinical application as a permeability marker in patients. The basis principle is to use a Gd-DTPA infusion and to assume that the input function to the brain is represented by the Gd-DTPA concentration in the femoral artery. The further assumption was made that during the upslope of the enhancement curve, the transport of the molecule is unidirectional, ie, from the intravascular space into the tumor and not vice versa. In reality, more likely a two directional exchange between the vascular compartment and the interstitium occurs, with the passage from the vascular compartment into the interstitium being greater during the upslope of the curve, resulting in a net transport of Gd-DTPA from the intravascular space into the ECF space of tumors. The opposite probably occurs during the downslope, showing the washout of Gd-DTPA from the tumor.

For practical purposes, Gd-DTPA may be more suited to measure permeability of brain tumors than the larger molecules which, at least theoretically, could also be used. Since the blood-to-tissue transport of these agents is much slower, as shown by our experiments, in our brain tumor model (and probably also in other brain tumors), the observation time to measure this process would be long. This in turn would result in a relatively long imaging time that may not be tolerated easily. The larger agents may be more useful in organs that do not have a BBB and are more "leaky."

The blood-to-tissue transport constant K_i was determined based on empirical calibration functions that correlate tissue [Gd-DTPA] concentration as a function of tumor MR image enhancement. The calculated K_i value was significantly lower for animals studied at 11 days postimplantation compared to the two animals studied at 15 days postimplantation. The increasing K_i with tumor age may reflect increasing neovascularity with abnormal vessels, known to occur with tumor growth. The validity of our approach is further supported by the fact that the mean K_i determined in tumors at 15 days post-tumor implantation using MR does not differ significantly from the mean K_i ($\pm$SEM) of 11.3 ± 1.7 mL/kg·min for the same time period determined by Spence et al in the identical tumor model using quantitative autoradiography (6, 19).

The wide confidence intervals of our calculated K_i values probably reflect uncertainty in the estimation of tissue [Gd-DTPA] from image enhancement. These intervals could be narrowed significantly if the function determining the dependence of enhancement on tissue [Gd-DTPA] were better known. The acquisition of additional data for the tissue Gd-DTPA concentration vs enhancement would be helpful but obviously cannot be achieved noninvasively. Others that used MR measurement of changes in T1 and T2 following injection of Gd-DTPA to determine permeability of multiple sclerosis lesions have encountered similar problems concerning the nonlinearity between local tissue Gd-DTPA concentration and signal intensity (20).

The approach to measure T1 values to assess BBB permeability has been investigated by others (20). One—at least theoretical—disadvantage of measuring T1, as opposed to measuring signal intensity by simply placing ROIs, is the time requirement to accurately measure T1 changes by using conventional SE or inversion recovery sequences. Since contrast media distribution is a very dynamic

process, an additional error would be introduced. Also, for practical purposes and potential clinical use, it is quite simpler to measure signal intensity than T1.

The intercept in Figure 8, which in theory reflects the plasma volume (per unit tumor mass), plus any additional volume for which [Gd-DTPA] is in rapid equilibrium with the plasma was negative for three of our A_t/C_{pt} vs. $\int_0^t C_{pt'}dt'/C_{pt}$ plots. Obviously, this intercept should be greater than zero. It has been suggested, however, that the Patlak method may be less than ideal for determining plasma volumes of tissues and the unexpected results in our measurements may reflect this (9). Furthermore, while this method appears well suited to measurement of K_i, the equilibration of Gd-DTPA within the ECF further contributes to the erroneous tumor plasma volume determination with our approach.

Multiple autoradiographic studies of blood-to-tissue transport in a variety of small animal brain tumors, both glial and metastatic, have been published (19, 21–24). Although the capillary permeability-surface area product (PS) is increased over normal brain tissue in many of these tumor models, there is a great deal of variability among the different models, among individuals with one tumor type, and even within individual tumors (19, 21–24). However, one common feature is that, in these tumors, it is primarily the PS product, and not regional blood flow, which limits the transport of drug-sized, water-soluble molecules from blood-to-brain tissue (6, 19). The degree of disruption of the BBB is not sufficient to allow rapid distribution of such molecules from the plasma to the tissue. Studies of a variety of primary and metastatic brain tumors in humans, using positron emission tomography with ^{68}Ga-EDTA as a tracer, support the finding that PS is often increased over normal values in brain tumors, but is highly variable among tumor types, and among patients with the same tumor type (18, 25).

The great variability in BBB permeability among individuals with brain tumors underlines the importance of determining the PS product in the clinical setting to optimize delivery of chemotherapeutic agents to tumor tissue. It has also been documented that radiation therapy changes the vascular permeability of brain tumors (6). Measurement of the PS may, therefore, also be helpful to optimize combined radiation and chemotherapy in patients with brain tumors (26, 27). In the postoperative setting, the differential diagnosis between recurrent or residual tumor and postoperative benign changes often remains unanswered by imaging modalities. If focal enhancement in a postoperative defect could be reliably quantitated and measured at different points in time following surgery, differentiation between recurrent or residual tumor and benign changes may be possible.

In summary, our results demonstrate that the tumor enhancement kinetic is dependent on the molecular size of the contrast agent used. We further demonstrate that the blood-to-tissue transport of Gd-DTPA can be used to quantitate BBB permeability using MR. This suggests that contrast-enhanced MR may be applicable to provide measurements of BBB permeability in the diagnosis and follow-up of patients with brain tumors.

Acknowledgment: The authors would like to thank G. Schuhmann-Giampieri, PhD, Institute for Contrast Media Research, Schering AG, Berlin, Germany and Alexander M. Spence, MD, Department of Neurology, University of Washington, Seattle, WA for their support of this work.

Note: Results indicating the potential of using MR signal enhancement to quantitate blood-to-tissue transport of Gd-DTPA in brain gliomas are considered pilot data. These data are part of a more detailed investigation. The manuscript describing this study is in preparation.

Appendix: BBB permeability was calculated using the graphical method of Patlak et al (9).

The accumulation of Gd-DTPA in tissue is described by

$$dA_t/dt = K_iC_{pt} + V_idC_{pt}/dt$$

where A_t = the tissue [Gd-DTPA] at time t, C_{pt} = the plasma [Gd-DTPA] at time t, and V_i = the plasma volume per unit mass of tissue, plus the volume of tertiary spaces for which Gd-DTPA exchange with the plasma is rapid. At time t, the tissue concentration of Gd-DTPA is given by:

$$A_t = K_i \int_0^t C_{pt'}dt' + V_iC_{pt}$$

Thus,

$$A_t/C_{pt} = K_i \int_0^t C_{pt'}dt'/C_{pt} + V_i$$

For each postcontrast image (at time t), A_t is calculated based on tumor enhancement, using the tissue calibration curve. The assumption is made that C_{pt} varies linearly with time between measurements. On the plot of A_t/C_{pt} vs $\int_0^t C_{pt'}dt'/C_{pt}$, K_i is the slope of the initial, linear portion of this plot, V_i is the intercept of this linear region. The plasma volume per unit mass of tissue was not expected to be reliably determined using Gd-DTPA, because this contrast agent distributes both within the intravascular and interstitial fluid space.

References

1. Sage MR. Blood-brain barrier: phenomenon of increasing importance to the imaging clinician. *AJR* 1982;138:887–898
2. Lidinsky WA, Drewes LR. Characterization of the blood-brain barrier: protein composition of the capillary endothelial cell membrane. *J Neurochem* 1983;41:1341–1347
3. Long DM. Capillary ultrastructure and the blood-brain barrier in human malignant brain tumors. *J Neurosurg* 1970;32:127–144
4. Torack RM. Ultrastructure of capillary reaction to brain tumors. *Arch Neurol* 1961;5:86–98
5. Schmiedl U, Maravilla KR, Nelson JA. Improved method for in vivo MR contrast media research. *Invest Radiol* 1991;26:65–70
6. Spence AM, Graham MM, O'Gorman LA, Muzi M, Abbott GL, Lewellen TK. Regional blood-to-tissue transport in an irradiated rat glioma model. *Radiot Res* 1987;111:225–236
7. Spence AM, Coates PW. Scanning electron microscopy of cloned astrocytic lines derived from ethylnitrosourea-induced rat gliomas. *Virchows Arch (B)* 1978;28:77–85
8. Ogan MD, Schmiedl U, Moseley ME, Grodd W, Paajanen H, Brasch RC. Albumin labeled with Gd-DTPA: an intravascular contrast-enhancing agent for MR blood pool imaging: preparation and characterization. *Invest Radiol* 1987;22:665–671
9. Patlak CS, Blasberg R, Fenstermacher J. Graphical evaluation of blood-to-brain transfer constants from multiple-time uptake data. *J Cereb Blood Flow Metab* 1983;3:1–7
10. Price AC, Runge VM, Nelson KL. CNS neoplastic disease. In Runge VM, ed. *Enhanced magnetic resonance imaging.* St. Louis: Mosby, 1989:139–177
11. Brant-Zawadzki M, Berry I, Osaki L, Brasch R, Murovic J, Norman D. Gd-DTPA in clinical MR of the brain. I. Intraaxial lesions. *AJR* 1986;147:1223–1230
12. Schmiedl U, Ogan MD, Paajanen H, et al. Albumin labeled with Gd-DTPA: an intravascular, blood-pool-enhancing agent for MR imaging: biodistribution and imaging studies. *Radiology* 1987;162:205–210
13. Wikström MG, Moseley ME, White DL, et al. Contrast-enhanced MR of tumors: comparison of Gd-DTPA and a macromolecular agent. *Invest Radiol* 1989;24:609–615
14. Petterson H, Appelgren L, Lundborg G, et al. Capillary permeability of two transplantable rat tumors as compared with various normal organs of the rat. In: *7th European Conference Microcirculation, Aberdeen 1972, Part II.* Biblanat. Basel, Switzerland: Karger; 1973:511–518
15. Vogler H, et al. Presented at the 17th International Congress of Radiology, Paris 1989, p. 972.
16. Kornguth S, Anderson M, Turski P, et al. Glioblastoma multiforme: MR imaging at 1.5 and 9.4 T after injection of polylysine-(Gd-DTPA) in rats. *AJNR* 1990;11:313–318
17. Kornguth SE, Kalinke T, Robins HI, Coghen JD, Turski P. Preferential binding of radiolabeled polylysines to C6 and U87 MG glioblastomas compared with endothelial cells in vitro. *Cancer Res* 1989;49:6390–6395
18. Hawkins RA, Phelps M, Huang SC, et al. Kinetic evaluation of blood-brain barrier permeability in human brain tumors with [68-Ga]EDTA and positron computed tomography. *J Cereb Blood Flow Metab* 1984;4:507–515
19. Spence AM, Graham MM, Abbot GL, Muzi M, Lewellen TK. Blood flow changes following 137-Cs irradiation in a rat glioma model. *Radiot Res* 1988;115:586–594.
20. Larsson H, Stubgaard M, Fredriksen J, Jensen M, Henriksen O, Paulson O. Quantitation of blood-brain barrier defect by magnetic resonance imaging and gadolinium-DTPA in patients with multiple sclerosis and brain tumors. *Magn Reson Med* 1990;16:117–131
21. Blasberg RG, Shapiro WR, Molnar P, Patlak CS, Fenstermacher JD. Local blood-to-tissue transport in walker 256 metastatic brain tumors. *J Neurooncol* 1984;2:205–218
22. Blasberg RG, Molnar P, Groothuis D, Patlak C, Owens E, Fenstermacher J. Concurrent measurements of blood flow and transcapillary transport in avian sarcoma virus-induced experimental brain tumors: implications for chemotherapy. *J Pharm Exp Ther* 1984;231:724–735
23. Yamada K, Hayakawa T, Ushio Y, Arita N, Kato A, Mogami M. Regional blood flow and capillary permeability in the ethylnitrosourea-induced rat glioma. *J Neurosurg* 1981;55:922–928
24. Groothuis DR, Molnar P, Blasberg RG. Regional blood flow and blood-to-tissue transport in five brain tumor models. *Prog Exp Tumor Res* 1984;27:132–153
25. Ianotti F, Fieschi C, Alfano B, et al. Simplified, noninvasive PET measurement of blood-brain barrier permeability. *J Comput Assist Tomogr* 1987;11:390–397
26. Brooks DJ, Beany RP, Thomas DG. The role of positron emission tomography in the study of cerebral tumors. *Semin Oncol* 1983;13:83–93
27. Jarden JO, Dhawan V, Poltorak A, Posner JB, Rottenberg DA. Positron emission tomographic measurement of blood-to-brain and blood-to-tumor transport of 82-Rb: the effect of dexamethasone and whole brain radiation therapy. *Ann Neurol* 1985;18:636–646